RSC Advances

PAPER

View Article Online
View Journal | View Issue

Cite this: *RSC Adv.*, 2018, **8**, 7615

Highly stretchable, mechanically stable, and weavable reduced graphene oxide yarn with high NO_2 sensitivity for wearable gas sensors†

Yong Ju Yun,[a] Do Yeob Kim,[b] Won G. Hong,[c] Dong Han Ha,[d] Yongseok Jun[a] and Hyung-Kun Lee*[be]

Stretchable gas sensors are important components of wearable electronic devices used for human safety and healthcare applications. However, the current low stretchability and poor stability of the materials limit their use. Here, we report a highly stretchable, stable, and sensitive NO_2 gas sensor composed of reduced graphene oxide (RGO) sheets and highly elastic commercial yarns. To achieve high stretchability and good stability, the RGO sensors were fabricated using a pre-strain strategy (strain-release assembly). The fabricated stretchable RGO gas sensors showed high NO_2 sensitivity (55% at 5.0 ppm) under 200% strain and outstanding mechanical stability (even up to 5000 cycles at 400% applied strain), making them ideal for wearable electronic applications. In addition, our elastic graphene gas sensors can also be woven into fabrics and clothes for the creation of smart textiles. Finally, we successfully fabricated wearable gas-sensing wrist-bands from superelastic graphene yarns and stretchable knits to demonstrate a wearable electronic device.

Received 24th November 2017
Accepted 10th February 2018

DOI: 10.1039/c7ra12760j

rsc.li/rsc-advances

1. Introduction

In recent years, stretchable electronics have attracted much attention as they offer the potential to overcome existing challenges in flexible/wearable electronics.[1] In particular, research focuses include increasing the stability of the electrical properties under various environmental deformations and improving the stretchability to achieve significant improvements in device performance, thereby opening up opportunities in wearable and soft electronics. For example, a variety of stretchable electronic materials have been prepared using ultrathin wavy silicone structures and serpentine meshes,[1–3] kirigami structures,[4] nanomaterial-based composites,[5–10] and ionogel and liquid metals.[11,12] Among these advanced materials, stretchable electronic fibers (e-fibers) have been widely developed as they are light-weight and low-cost, and have the ability to be woven and knitted.[13–15]

Recently, graphene-based e-fibers have attracted attention as promising stretchable electronic materials for wearable electronics due to high electrical conductivity, excellent elasticity, outstanding chemical and thermal stability, and good biocompatibility.[16] In particular, reduced graphene oxide (RGO)-based e-fibers offer additional advantages, such as versatility in chemical functionalization, simple solution-based processing, mass production, and relatively low cost. Based on these advantages, stretchable RGO e-fibers with high reliability have been developed for various wearable device applications, such as stretchable electrical conductors, supercapacitors, strain sensors, and actuators.[17–20] However, to date, there have been no reports of highly stretchable gas sensors based on graphene fibers with good stability and reliability.

Here, we fabricated highly stretchable, mechanically stable, and weavable RGO elastic electronic yarns (e-yarns) using dip-coating with the pre-strain strategy and demonstrated wearable wrist-band gas sensors. The RGO e-yarns were made from electro-conductive RGO flakes and commercial spandex/polyester core-spun elastic yarns. They exhibited a superior stretchability (up to 400%) and mechanical stability (up to 5000 cycles of repeated stretch-release) and high NO_2 sensitivity under 200% strain at room temperature. In addition, these e-yarns can be easily sewn or woven into soft clothes by commercial weaving and knitting techniques without any difficulties. Using these stretchable gas sensors with unique properties, we demonstrated that the highly NO_2 sensitive RGO

[a]*Department of Energy Engineering, Konkuk University, Seoul, 05029, Republic of Korea*

[b]*ICT Materials & Components Research Laboratory, Electronics and Telecommunications Research Institute, Daejeon, Republic of Korea. E-mail: hklee@etri.re.kr*

[c]*Division of Electron Microscopy Research, Korea Basic Science Institute (KBSI), Daejeon, 34133, Republic of Korea*

[d]*Quantum Technology Institute, Korea Research Institute of Standards and Science (KRISS), Daejeon, 34113, Republic of Korea*

[e]*Department of Advanced Device Technology, University of Science & Technology, Daejeon, Republic of Korea*

† Electronic supplementary information (ESI) available. See DOI: 10.1039/c7ra13387a

gas sensors could be integrated into a wearable gas sensing device, which could be used by citizens or workers for real-time monitoring of harmful gas. We believe that our stretchable graphene gas sensor is a highly promising material for the development of next-generation environmental applications for the "internet of things" (IoT).

2. Experimental sections

2.1 Materials

Graphite powder (SP-1 graphite) was purchased from Bay Carbon (Michigan, USA). Bovine serum albumin (BSA) powder, hydroiodic acid (HI), sodium acetate ($NaC_2H_3O_2$), and sodium bicarbonate ($NaHCO_3$) were purchased from Sigma-Aldrich (Korea). Spandex-polyester core-spun yarns were purchased from J&J Textile Co. (Korea).

2.2 Fabrication of RGO elastic yarns

A GO solution was synthesized using a modified Hummer method.[21] A colloidal solution of GO flakes in deionized (DI) water with a concentration of 1 mg mL^{-1} was prepared using an ultrasonicator (Q-700, Qsonica, LLC.). For amine-functionalization, commercial elastic yarns (EYs) were incubated in a vessel with BSA solution for 30 min at room temperature. After treatment, the BSA-coated EYs (BSAEYs) were rinsed with DI water followed by drying under a flow of nitrogen. GO flakes were coated onto pre-strained BSAEYs for 10 min under mild stirring. The RGO elastic yarn samples prepared without stretching are henceforth referred to as RGOEY; these samples were prepared in exactly the same way as the pre-strained (FRGOEY) samples, but without pre-straining. A home-made vessel for GO coating was used to mechanically stretch the EYs to a pre-strain of 400%. This process was repeated as required to obtain the desired number of GO coatings. After GO coating, the GO-coated EYs (GOEYs) were chemically reduced with HI (10 mL)/sodium acetate (SA) (10 mL) solutions for 30 min at 50 °C. To neutralize and remove residues of hydriodic ions on RGO, the sample was first immersed in 200 mL sodium bicarbonate solutions for 3 h and then immersed in 1 L DI water for 10 h. The resulting RGO yarns are referred to as FRGOEY-*n* based on the number of GO coating (where *n* is the number of GO dip-coating steps).

2.3 Characterization and measurements

The surface morphology of all samples was analyzed using field-emission scanning electron microscopy (FESEM; Hitachi SU8200, Japan). Raman spectra were acquired using a micro-Raman system (LabRAM HR, HORIBA Scientific) with an excitation energy of 2.33 eV and an excitation wavelength of 532 nm. X-ray photoelectron spectroscopy (XPS) measurements were taken by a ESCALAB 200R (Thermo VG Scientific) using a monochromatic Al-Kα X-ray source at 250 W. Tensile tests were performed using Instron 5567A. The electrical properties were characterized in air with a B2901A source measurement unit (Keysight Technologies). Resistance changes of the elastic RGO yarns were measured at room temperature (22–24 °C) using a digital multimeter (Agilent 34970A) and a Benchlink data logger program. Dry balance gas and wet balance gas were mixed using mass flow controllers in appropriate ratios to control the relative humidity. The relative humidity was measured using a commercial humidity sensor (Sensirion SHTC1).

2.4 Durability to stretching

Samples of the stretchable RGO e-yarns (FRGOEYs and RGOEYs) with a length of 3 cm were placed in a computer-controlled and motorized actuating system (built in house) for repeated stretch-release tests. One end of the sample was attached to a fixed stage and the other end was fixed to a movable stage. Durability tests were performed up to 5000 cycles with a scan rate of 1.0 cm s^{-1} under various strains from 0 to 400%. The electrical characteristics of the sample were simultaneously measured using a 34461A digital multimeter (Keysight Technologies).

3. Results and discussion

We used the pre-strain strategy to fabricate stretchable RGO e-yarns as this method has been shown to produce yarns with stable behavior.[9,22] The key fabrication process is schematically illustrated in Fig. 1, where GO coating of pre-strained EY and low-temperature chemical reduction are shown. We used commercial EY comprised inelastic polyester yarn (PY; light blue) and elastic spandex yarn (SY; gray) that can stretch up to a maximum strain of 400% (Fig. 1a(i) and S1†). In addition, the PY consisted of a bundle of microfibers with an average diameter of 18 μm. Although a single PY is non-stretchable, the EYs in the covered forms can be stretched up to 400%. The EYs were functionalized with BSA molecular glues (yellow) *via* dip-coating, which induced positive charges on the surface of the EYs (Fig. 1a(ii)).[23] The BSA serves as a universal adhesive for improving the adsorption of GO flakes onto the EY surface.

Subsequently, the BSAEYs pre-strained at 400% strain were then dipped in an aqueous 1 mg mL^{-1} GO solution (Fig. 1a(iii)). A coating of GO sheets (brown) was formed on the BSAEYs through electrostatic self-assembly (Fig. 1a(iv)). Finally, the as-prepared FGOEY was chemically reduced by immersing it in the HI/SA solution (Fig. 1a(v)). For the RGOEY reference samples, GO flakes were coated onto the BSAEYs without pre-straining (Fig. 1(vi) and (vii)). More details about the sample preparation and characterizations are provided in the ESI.†

Fig. 1b shows photographs of the FRGOEY before and after release of the stretching. The color of the EYs changed from white to black during the GO wrapping and the chemical reduction process. The FRGOEY is comprised of both RGO-coated spandex yarn (FRGOSY) as a stretchable backbone with a diameter of 50 μm and RGO-coated polyester yarn (FRGOPY) as a sensing channel with a diameter of 200 μm, as shown in the FESEM image in Fig. 1c. The high magnification image (inset) shows numerous wrinkles on the surface of FRGOPY, which was attributed to the successful coating of RGO sheets onto the PY surfaces. The FRGOEYs were further characterized using micro Raman spectroscopy. Fig. 1d shows Raman spectra of EY,

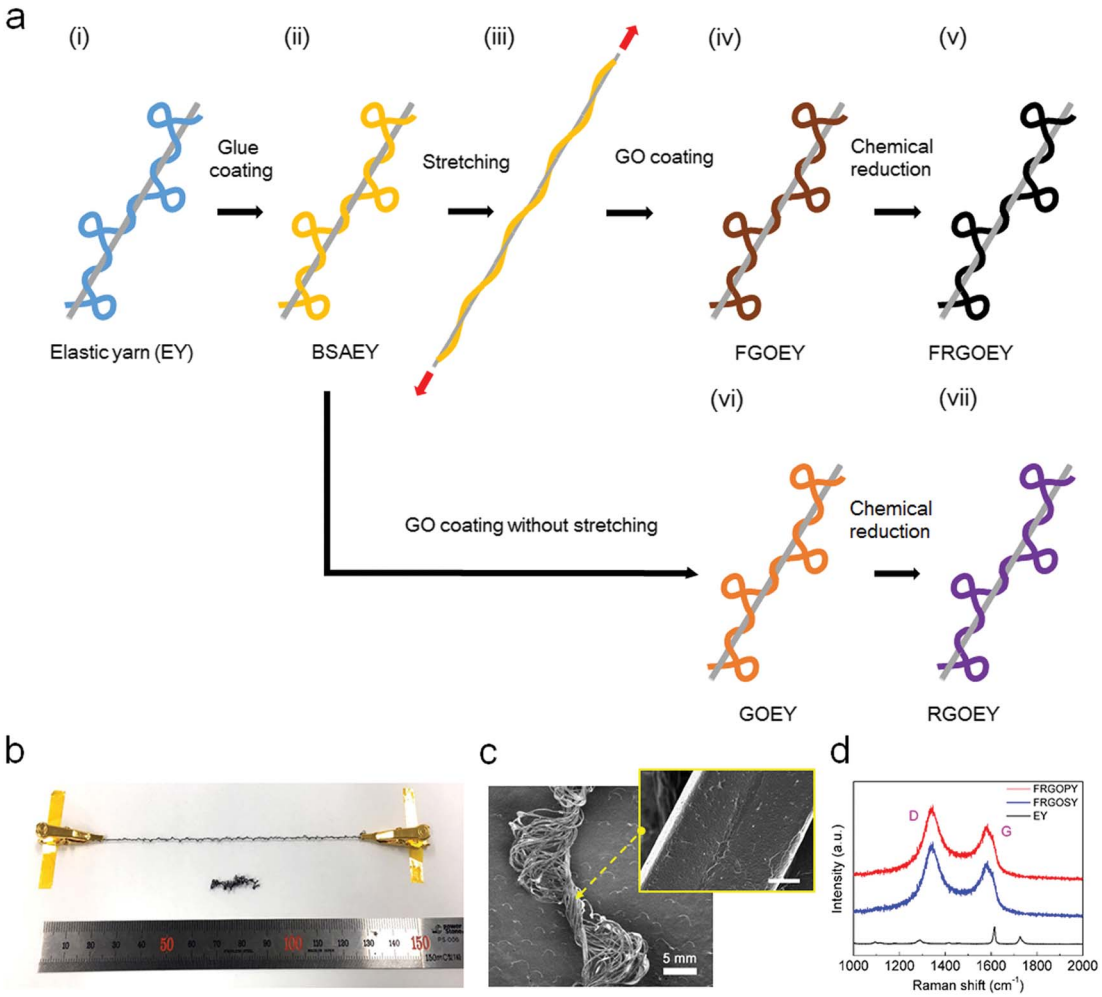

Fig. 1 (a) Schematic illustration of the preparation of stretchable graphene electronic yarns (FRGOEY and RGOEY). (b) A photograph of the FRGOEY with and without 400% stretching. (c) FESEM image of the FRGOEY. Inset: high-resolution FESEM image of the FRGOEY (scale bar: 5 μm). (d) Raman spectra of FRGOEY. FRGOEY is composed of RGOPY and RGOSY. EY (elastic yarn; dark) is core-spun spandex-polyester yarn.

FRGOPY, and FRGOSY. After GO coating and chemical reduction, the Raman spectra of both FRGOPY and FRGOSY exhibited typical RGO spectral features, such as the D peak at 1340 cm^{-1} and the G peak at 1580 cm^{-1}, which were nearly identical to those of an RGO film (Fig. S2†).[24] Fig. S3† also shows Raman spectra of various areas of a single FRGOEY. This indicates that the RGO sheets were successfully coated on the surface of the FRGOEY. Both FGOEY and FRGOEY were further characterized using XPS. Curve fitting of the XPS spectra was performed using a Gaussian–Lorentzian peak shape after performing a linear background correction. Fig. S4a and b† show the XPS spectra of XPS C1 spectra of FGOEY and FRGOEY. The peaks of C 1s in the FGOEY were composed of the C–C (284.6 eV), C–N (285.81 eV), C–O (286.66 eV), C═O (287.65 eV), and C(O)O (288.56 eV) species. The chemical evolution of FRGOEY was confirmed through a diminished O 1s/C 1s ratio and based on the reduced intensity of the oxygen-containing group in the XPS C 1s core-level spectra as compared to FGOEY.

Fig. 2a shows initial resistance values of FRGOEY-1, FRGOEY-2, RGOEY-1, and RGOEY-2, as measured using the two-probe method. The optimized chemical reduction time was 30 min (Fig. S5†). With increasing number of RGO coatings, the electrical resistance of all samples decreased (Fig. 2a). This result indicates that percolating conducting pathways were formed on the surface of the EYs due to the thicker electro-conductive RGO layer. Furthermore, both FRGOEY samples showed lower resistance values compared than those of the RGOEYs, indicating that more effective electron percolation pathways were formed with pre-straining. As a stretchable electronic material, the EY consisted of two kinds of electro-conductive RGO yarns (RGOSY and RGOPY) and had unique stretching properties because of the different characteristics of each yarn. Since RGOSY has much higher elasticity (Fig. S6a†), their stretch-release behavior is mainly governed by the elastic properties of the RGOSY. However, after the first stretch-release cycle at 50% strain, they showed insulating behavior (Fig. S6b†). Therefore, the electrical properties of both stretchable FRGOEYs and RGOEYs depended on the morphology of the RGOPYs. Although the resistance values of all samples increased through the first stretch-release cycle, the values stabilized thereafter (Fig. 2b). The mechanical strength was also measured for FRGOEY, which was compared with its pristine

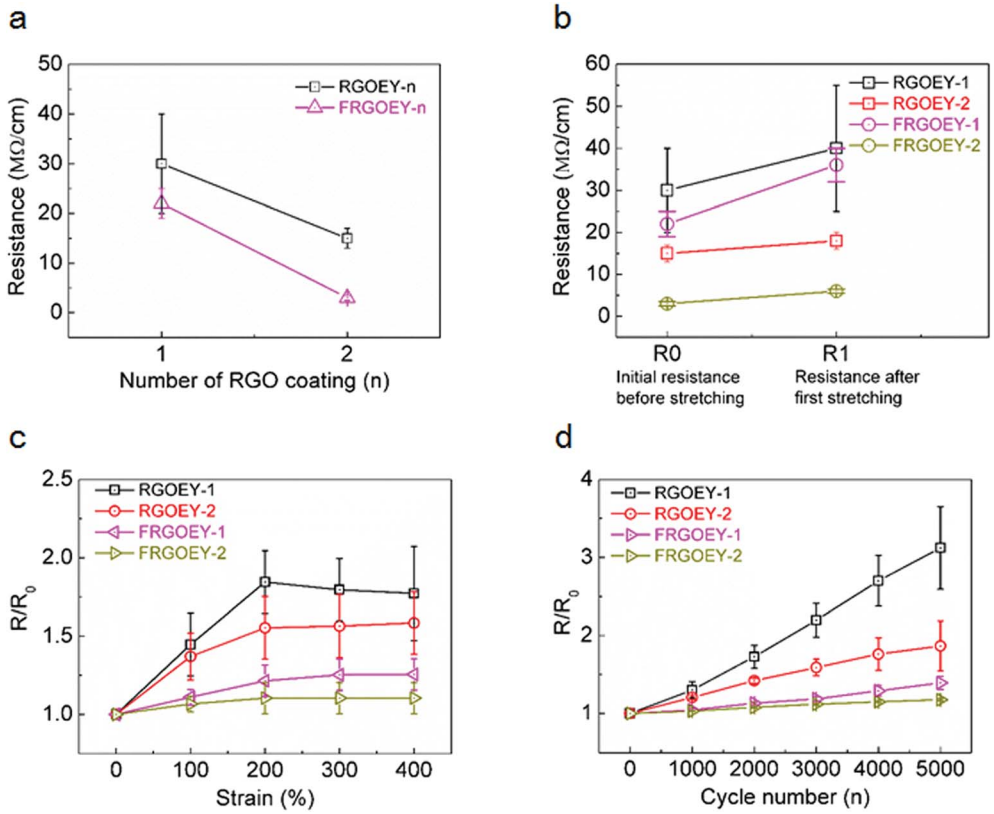

Fig. 2 (a) Electrical resistance of RGOEY-1, RGOEY-2, FRGOEY-1, and FRGOEY-2 as a function of number of RGO coatings. The average resistance values of the samples were calculated for ten specimens for each sample and the error bars denote the standard deviation. (b) Relative variations in resistance of four samples up to 400% strain in the first stretch-release cycle. (c) Resistance *vs.* strain for RGOEY-1 (black square), RGOEY-2 (red circle), FRGOEY-1 (pink triangle), and FRGOEY-2 (dark yellow triangle). (d) Relative variations in resistance over 5000 repeated stretch-release cycles at 400% strain.

material (Fig. S7†). The tensile strengths and strains are 57.6 MPa, 713% for EY and 61.7 MPa, 710% for FRGOEY, respectively. Mechanical properties of FRGOEY are nearly identical with those of EY.

The highly stretchable graphene yarns were tested for their usability as stretchable e-textiles. Fig. 2c shows the resistance changes (R/R_0, where R is the measured resistance and R_0 is the original resistance before stretching) of FRGOEYs and RGOEYs as a function of tensile strain. Interestingly, the resistance of all samples increased from the beginning of stretching to 200% strain and then remained steady or decreased slightly. These differences in electrical resistance reveal two different mechanisms affecting the resistance under stretching. These results can also be explained by examining the structural changes of the RGOEYs under stretch-release cycles (Fig. S8†). Stretching tests were performed using a tensile stage while observing the samples with an optical microscope. Before stretching, the RGOEYs exhibited the typical structure of spandex/polyester core-spun yarn (Fig. S8,† 0% strain). During stretching, the electrically conducting RGOPY morphologies changed from large circles with a radius of curvature of 2.0 ± 1.0 mm to small circles with a radius of curvature of 1.0 mm (Fig. S8,† 100% strain). Therefore, stretching of the RGOPY reduced intersheet connections of the coated electro-conductive RGO flakes (Fig. S8,† 100% strain). This weakened percolation consequently increased the electrical resistance of the RGOPY. When the RGOEYs were stretched beyond 200% strain, the coiled RGOPY were straightened along the stretching direction. However, the resistance values remained steady or slightly decreased due to the remaining twist in the structure (Fig. S9†). Therefore, the variations in the electrical resistance can be attributed to the contact between individual RGO flakes on the surface of the RGOPYs during the stretching process.

The mechanical stability is a critical factor affecting the reliability of e-textiles for practical applications in wearable electronics. The stability of the RGO e-yarns was investigated through repeated stretch-release cycling tests. Fig. 2d shows the resistance changes under repeated stretch-release cycling tests. Compared with the RGOEYs without pre-straining, the FRGOEYs possessed good stretchability and mechanical stability. For both FRGOEY-1 and FRGOEY-2, the output signal remained stable without any significant degradation during long-term cycling; this indicates the excellent mechanical stability of the e-yarn under severe deformation. These outstanding electrical properties and reliability under mechanical stress have made it possible to utilize such materials in a wide variety of stretchable electronic devices, such as electronic interconnects and conductors, physical and chemical

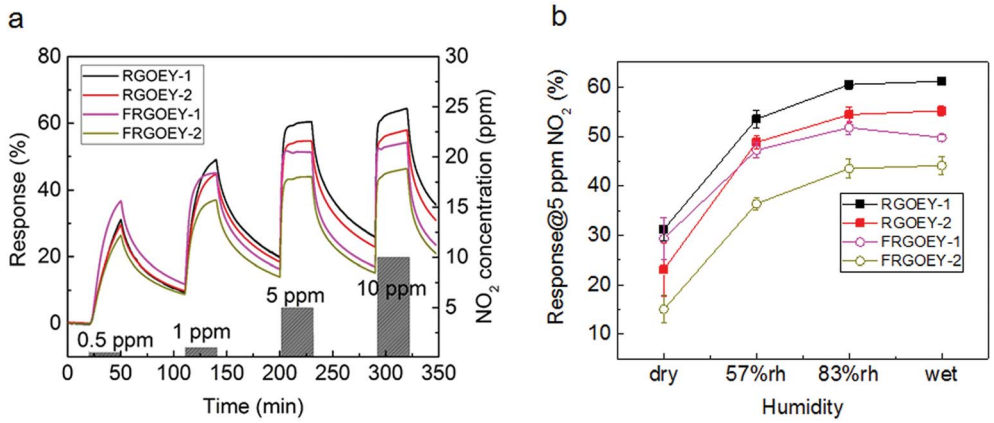

Fig. 3 (a) Gas sensing performances of RGOEY-1, RGOEY-2, FRGOEY-1, and FRGOEY-2 exposed to 0.5 ppm, 1.0 ppm, 5.0 ppm, and 10.0 ppm NO_2 gas at room temperature under wet conditions. (b) Gas sensing performances of RGOEY-1, RGOEY-2, FRGOEY-1, and FRGOEY-2 exposed to 5.0 ppm NO_2 gas under dry air, 57% RH, 83% RH, and wet conditions.

sensors, actuators, and energy device electrodes.[13,15,17–20,25] The utility of the stretchable conductivity was demonstrated in advancing chemical gas sensors toward stretchable forms.

Based on their promising electrical characteristics, RGOEYs and FRGOEYs were investigated here for NO_2 gas sensing applications; this gas is a notorious environmental pollutant. The concentration range of NO_2 for the experiments was from 500 parts-per-billion (ppb) to 10 parts-per-million (ppm) (Fig. 3a). The RGOEY and FRGOEY were exposed to NO_2 gas under different relative humidity conditions and elongation strains. The sensor response was defined as $S\,(\%) = (R_a - R_g)/R_a \times 100$, where R_a and R_g denote the electrical resistance upon exposure to air and the analyte gas, respectively. The RGOEY and FRGOEY samples showed different responses depending on the number of RGO coatings on the fiber, which showed that even the smallest amount of sensing material was effective for giving a high response to NO_2 gas.[26] When the fibers were exposed to oxidant gas such as NO_2, the RGO sensing material interacted with NO_2 by donating electrons to the oxidant gas, resulting in a decrease in its resistance due to p-type semiconducting behavior.[27,28] As expected, the mechanism of gas-sensing of NO_2 on the stretchable graphene electronic yarns in this research is considered to be not much different from the others based on graphene and its derivatives because the sensing materials are similar. The graphene in this research provides a firm adhesion resulting from 2D material characteristics of the graphene. This advantage contributes to a reproducible and reliable sensing property under the stretchable circumstance. The RGOEY sample showed higher sensitivity to NO_2 compared to FRGOEY over the entire measured concentration range, except for 500 ppb. As FRGOEY was coated with GO under full elongation, it was coated by a larger amount of sensing materials due to an increased surface area compared to the RGOEY, which resulted in the relatively reduced response of FRGOEY. However, FRGOEY showed high performance regarding the response/recovery times (Fig. S10†). The response time is defined as the time for a sensor to respond to an introduced gas from 0 to 90% response. The recovery time is defined as the time from 100% to 10% response when the gas is removed. FRGOEY-1 showed a response time of 1.9 min under exposure to 5.0 ppm NO_2; this is remarkable compared to the several tens of minutes required by most RGO-based gas sensors at room temperature.[29,30] As shown in Fig. S10,† the recovery time was in the range of around 40 min. However, the recovery time could be reduced by a third by exposing the samples to UV irradiation at 365 nm (Fig. S11†).

SEM observations (Fig. S12†) showed that most of the RGO coated on the elastic yarn was adhered to the polyester and the

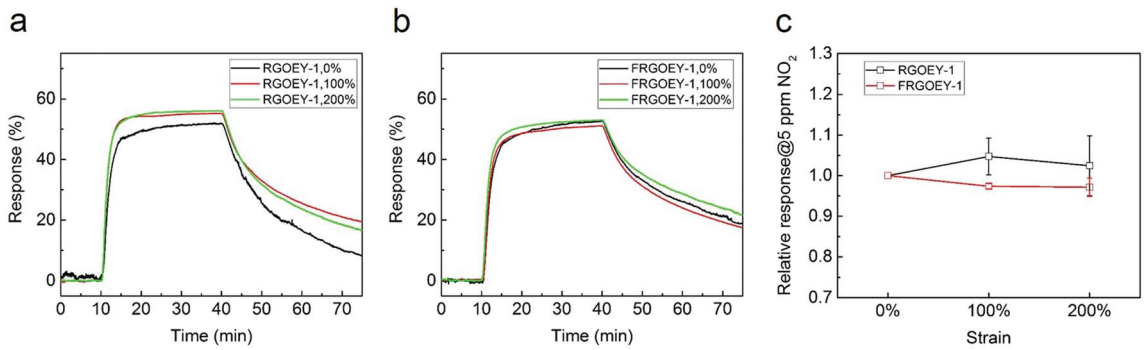

Fig. 4 (a and b) Gas sensing performances of RGOEY-1 and FRGOEY-1 exposed to 5.0 ppm NO_2 gas under 0%, 100%, and 200% strains. (c) Comparison of gas sensing performances of RGOEY-1 and FRGOEY-1 exposed to 5.0 ppm under 0%, 100%, and 200% strains.

Fig. 5 (a and b) Photographs of the wearable wrist-band integrated with the FRGOEY gas sensor. (c) Response of the wearable gas sensor wrist-band to 500 ppb of NO_2 at room temperature.

RGO on the spandex was removed during repeated stretch-release tests. The gas sensing behavior of the core-spun EY is thought to originate from the nature of the polyester yarn. Polyester is known to swell at a rate of 10^{-6}/% RH with increasing humidity.[31] The response is governed by the increase in accessible surface area in the relatively dry region. However, NO_2 molecules compete with water molecules on the RGO surface as humidity increases. These two effects on the response contribute to saturated responses in the wet condition by balancing each other (Fig. 3b).

Stretchable gas sensors have been reported based on several substrates, such as mogul-patterned PDMS, serpentine-patterned ecoflex, and electro-spun elastomeric nanofiber multilayers.[32–35] The previous work investigated the sensitivity of gas sensors with an external strain up to 50%. In this work, we investigated the resistance changes of the gas sensor with external strain up to 200%. The RGO e-yarns were placed in sample holders of the chamber that can stretch the samples by adjusting external metric knobs (Fig. S13†). RGOEY-1 and FRGOEY-1 showed a response of 50–55% to 5.0 ppm NO_2 with an external strain up to 200% (Fig. 4a and b) and the variation in the response under the external strain was within 5% of the changes based on the response without an external strain (Fig. 4c). Moreover, FRGOEY-1 exhibited more reliable responses (lower standard deviation) during measurements under the same strain than RGOEY-1, resulting from its superior mechanical stability (as shown in Fig. 2c and d).

To demonstrate the potential of the FRGOEY gas sensors in wearable electronics, we fabricated a wearable wrist-band gas sensor (Fig. 5a and b). The white wrist-band was knitted using a commercial knitting loom that can be stretched up to a maximum of 150% in the *x*-direction and up to a maximum of 200% in the *y*-direction (Fig. S14†). The wrist-band gas sensor composed of uncoated spandex yarn and FRGOEY exhibited a response of 25% to 500 ppb NO_2 under saturated humidity conditions, which is similar to the response of the FRGOEY shown in Fig. 3a.

4. Conclusions

We developed a new wearable gas sensor with high stretchability and good mechanical stability using a pre-straining method. The graphene e-yarns were successfully prepared by combining RGO flakes and commercial elastic yarns. The samples exhibited outstanding electrical properties and stability against repeated external stresses. In addition, the FRGOEY showed excellent gas-sensing performance (50–55% response to 5.0 ppm of NO_2 under 200% strain at room temperature), which is one of the most sensitive gas sensors among those known to date for stretchable applications. In addition, the FRGOEY-based gas sensor was integrated into a knitted wrist-band in the form of fabrics. Based on the remarkable performance of the RGO e-yarns, we believe that the developed high-performance gas sensor will provide new opportunities for the development of advanced materials and devices for next-generation wearable electronics.

Conflicts of interest

There are no conflicts to declare.

Acknowledgements

This research was supported by the National Research Foundation of Korea under research projects (NRF-2016R1A2B4007570), (NRF-2015M1A2A2056829), and (NRF-2017M3A9F1033056); the Ministry of Trade, Industry and Energy (MOTIE), Korea Institute for Advancement of Technology (KIAT) through the Encouragement Program for the Industries of Economic Cooperation Region (No. A01210053); and the KU Research Professor Program of Konkuk University.

References

1 D.-H. Kim and J. A. Rogers, *Adv. Mater.*, 2008, **20**, 4887–4892.
2 D.-H. Kim, N. Lu, R. Ma, Y.-S. Kim, R.-H. Kim, S. Wang, J. Wu, S. M. Won, H. Tao, A. Islam, K. J. Yu, T.-I. Kim, R. Chowdhury, M. Ying, L. Xu, M. Li, H.-J. Chung, H. Keum, M. McCormick, P. Liu, Y.-W. Zhang, F. G. Omenetto, Y. Huang, T. Coleman and J. A. Rogers, *Science*, 2011, **333**, 838–843.
3 M. L. Hammock, A. Chortos, B. C.-K. Tee, J. B.-H. Tok and Z. Bao, *Adv. Mater.*, 2013, **25**, 5997–6038.

4 T. C. Shyu, P. F. Damasceno, P. M. Dodd, A. Lamoureux, L. Xu, M. Shlian, M. Shtein, S. C. Glotzer and N. A. Kotov, *Nat. Mater.*, 2015, **14**, 785–789.
5 S. Yao and Y. Zhu, *Adv. Mater.*, 2015, **27**, 1480–1511.
6 T. Sekitani, Y. Noguchi, K. Hata, T. Fukushima, T. Aida and T. Someya, *Science*, 2008, **321**, 1468–1472.
7 D. J. Lipomi, M. Vosgueritchian, B. C.-K. Tee, S. L. Hellstrom, J. A. Lee, C. H. Fox and Z. Bao, *Nat. Nanotechnol.*, 2011, **6**, 788–792.
8 Y. Kim, J. Zhu, B. Yeon, M. D. Prima, X. Su, J.-G. Kim, S. J. Yoo, C. Uher and N. A. Kotov, *Nature*, 2013, **500**, 59–63.
9 P. Kang, M. C. Wang, P. M. Knapp and S. Nam, *Adv. Mater.*, 2016, **28**, 4639–4645.
10 Y. J. Yun, J. Ju, J. H. Lee, S.-H. Moon, S.-J. Park, Y. H. Kim, W. G. Hong, D. H. Ha, H. Jang, G. H. Lee, H.-M. Chung, J. Choi, S. W. Nam, S.-H. Lee and Y. Jun, *Adv. Funct. Mater.*, 2017, **27**, 1701513.
11 B. Chen, J. J. Lu, C. H. Yang, J. H. Yang, J. Zhou, Y. M. Chen and Z. Suo, *ACS Appl. Mater. Interfaces*, 2014, **6**, 7840–7845.
12 M. D. Dickey, *Adv. Mater.*, 2017, **29**, 1606425.
13 Z. F. Liu, S. Fang, F. A. Moura, J. N. Ding, N. Jiang, J. Di, M. Zhang, X. Lepro, D. S. Galvao, C. S. Haines, N. Y. Yuan, S. G. Yin, D. W. Lee, R. Wang, H. Y. Wang, W. Lv, C. Dong, R. C. Zhang, M. J. Chen, Q. Yin, Y. T. Chong, R. Zhang, X. Wang, M. D. Lima, R. Ovalle-Robles, D. Qian, H. Lu and R. H. Baughman, *Science*, 2015, **349**, 400–404.
14 J. Lee, H. Kwon, J. Seo, S. Shin, J. H. Koo, C. Pang, S. Son, J. H. Kim, Y. H. Jang, D. E. Kim and T. Lee, *Adv. Mater.*, 2015, **27**, 2433–2439.
15 Y. Wei, S. Chen, X. Yuan, P. Wang and L. Liu, *Adv. Funct. Mater.*, 2016, **26**, 5078–5085.
16 Z. Xu and C. Gao, *Mater. Today*, 2015, **18**, 480–492.
17 Z. Xu, Z. Liu, H. Sun and C. Gao, *Adv. Mater.*, 2013, **25**, 3249–3253.
18 S. Wang, N. Liu, J. Su, L. Li, F. Long, Z. Zou, X. Jiang and Y. Gao, *ACS Nano*, 2017, **11**, 2066–2074.
19 Y. Cheng, R. Wang, J. Sun and L. Gao, *Adv. Mater.*, 2015, **27**, 7365–7371.
20 H. Cheng, Y. Hu, F. Zhao, Z. Dong, Y. Wang, N. Chen, Z. Zhang and L. Qu, *Adv. Mater.*, 2014, **26**, 2909–2913.
21 W. S. Hummers and R. E. Offeman, *J. Am. Chem. Soc.*, 1958, **80**, 1339.
22 F. Xu, W. Lu and Y. Zhu, *ACS Nano*, 2011, **5**, 672–678.
23 Y. J. Yun, W. G. Hong, W.-J. Kim, Y. Jun and B. H. Kim, *Adv. Mater.*, 2013, **25**, 5701–5705.
24 D. H. Ha, S. Jung, H.-J. Kim, D. Kim, W.-J. Kim, S. N. Yi, Y. Jun and Y. J. Yun, *Synth. Met.*, 2015, **204**, 90–94.
25 C. Choi, J. M. Lee, S. H. Kim, S. J. Kim, J. Di and R. H. Baughman, *Nano Lett.*, 2016, **16**, 7677–7684.
26 Y. J. Yun, W. G. Hong, N. J. Choi, H. J. Park, S. E. Moon, B. H. Kim, K. B. Song, Y. Jun and H.-K. Lee, *Nanoscale*, 2014, **6**, 6511–6514.
27 Y. J. Yun, W. G. Hong, N. J. Choi, B. H. Kim, Y. Jun and H. K. Lee, *Sci. Rep.*, 2015, **5**, 10904.
28 U. Latif and F. L. Dickert, *Sensors*, 2015, **15**, 30501–30524.
29 J. D. Fowler, M. J. Allen, V. C. Tung, Y. Yang, R. B. Kaner and B. H. Weiller, *ACS Nano*, 2009, **3**, 301–306.
30 J. Zhang, X. Liu, G. Neri and N. Pinna, Nanostructured materials for room-temperature gas sensors, *Adv. Mater.*, 2016, **28**, 795–831.
31 O. Isuke, H. Masahiro and T. Takashi, *Jap. J. App. Phys.*, 1992, **31**, 2505–2507.
32 H.-B. Lee, C.-W. Bae, L. T. Duy, I.-Y. Sohn, D.-I. Kim, Y.-J. Song, Y.-J. Kim and N.-E. Lee, *Adv. Mater.*, 2016, **27**, 3069–3077.
33 J. Yun, Y. Lim, G. N. Jang, D. Kim, S.-J. Lee, H. Park, S. Y. Hong, G. Lee, G. Zi and J. S. Ha, *Nano Energy*, 2016, **19**, 401–414.
34 L. T. Duy, T. Q. Trung, A. Hanif, S. Siddiqui, E. Roh, W. Lee and N.-E. Lee, *2D Materials*, 2017, **4**, 025062.
35 D. C. Han, H. J. Shin, S. H. Yeom and W. Lee, *J. Sensor Sci. & Tech.*, 2017, **26**, 301–305.